

Density functional theory study of the structural and energetically properties of 1H-tetrazolyl cubane as high energy density material

Mehdi Nabati* and Mehrdad Mahkam

Chemistry Department, Faculty of Science, Azarbaijan Shahid Madani University, Tabriz, Iran.

Received: July 2014; Revised: July 2014; Accepted: July 2014

Abstract: The objective of this research is to design novel nitrogen-rich derivative of the cubane nucleus for use as energetic material. In present study, 1H-tetrazolyl cubane was designed and optimized to obtain molecular geometry and electronic structure at density functional theory (DFT, B3LYP) at the levels of 6-311G(d), 6-311G(d,p), 6-311G(2d,2p). Some important properties such as bond dissociation enthalpy, density, frontier orbital energy, thermodynamic parameters, natural bond orbital population, and heat of formation and detonation parameters were then calculated. Also, IR and NMR spectra of the structure were simulated. It observed that the tetrazolyl group can improve the detonation properties of cubane. The simulation results revealed that this compound exhibit excellent performance; and that is viable candidate of high energy density materials (HEDMs).

Keywords: 1H-tetrazolyl cubane, Energetic compound, Bond dissociation energy, Heat of formation, Detonation properties.

Introduction

Cubane, pentacyclo [4.2.0.0^{2,5}.0^{2,8}.0^{4,7}] octane, the important member of the family of 20 possible (CH)₈ species, was originally thought impossible to prepare. In 1964, Philip Eaton and his coworkers reported the first tactical synthesis of the cubane carbon skeleton [1]. And also, they synthesized the highly nitrated Cubans as high energy compounds in 2000 [2]. Cubane is a high strained system, and its' nitrogen-rich derivatives are energetic materials. The density and enthalpy of cubane are 1.29 g/cm³ and 144 kcal/mol, respectively [3]. Nowadays, cubane tetrazolyl derivatives weren't synthesized. In present work, we report the theoretical study of the 1H-tetrazolyl cubane as high energy density material. A particularly important method is to model a molecular system prior to synthesizing that molecule in the laboratory. This is very useful mean because synthesizing a compound

could need months of labor and raw materials, and generates toxic waste. A second use of computational chemistry is in understanding a problem more completely [4-6]. There are some properties of a molecule that can be obtained theoretically more easily than by experimental means. The density functional theory (DFT) methods are theoretical techniques for the prediction of structural and detonation properties of various chemical systems [7]. There are many DFT methods that have been used in the last few decades [8]. We have successfully used B3LYP method for computing geometry, bond dissociation energy, natural bond orbital population, surface density, frontier orbitals energy and heat of formation through isodesmic reactions.

Results and discussion

The geometry of 1H-tetrazolyl cubane:

There are many energetic compounds with most usages. Their classification is according to the types of

*Corresponding author. Tel: (+98) 413 4327501, Fax: (+98) 413 4327501, E-mail: mnabati@ymail.com

groups present in their structures like azides, nitro, nitramines etc. However, a look into the high energy density materials reveals that the nitrogen-rich rings are more responsible for the energy character of the molecules. Tetrazole, one of the major nitrogen-rich compounds, is a five membered ring with four nitrogen atom and one carbon atom. If the tetrazolyl group is linked to a carbon atom in cubane structure, the

detonation performance of the system could be increased by electron withdrawing property of the ring nitrogen atoms. The geometric structure of 1H-tetrazolyl cubane and its' atomic numbering is displayed in Figure 1. The dipole moment of the molecule at studied levels is listed in Table 1. As seen from the table, 1H-tetrazolyl cubane is a very polar system and its' dipole moment is six debye.

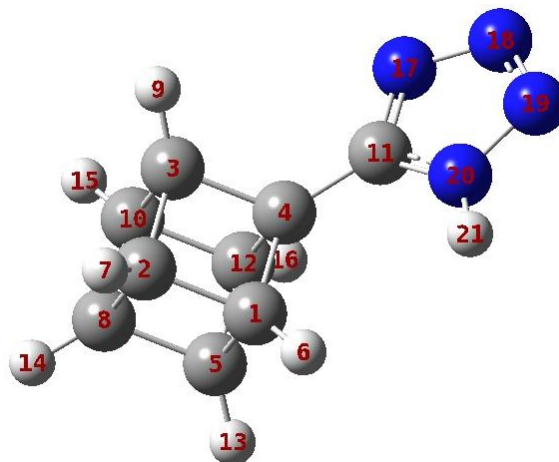


Figure 1: The geometric structure of 1H-tetrazolyl cubane with atomic numbering (White: H, Grey: C, Blue: N).

Table 1: Dipole moment of 1H-tetrazolyl cubane calculated at studied levels.

Methods	μ_x (Debye)	μ_y (Debye)	μ_z (Debye)	μ_{Tot} (Debye)
B3LYP/6-311G(d)	5.0473	3.4775	0.0000	6.1293
B3LYP/6-311G(d,p)	-5.0386	3.4489	-0.0001	6.1059
B3LYP/6-311G(2d,2p)	4.9035	3.3505	0.0000	5.9388

Bond lengths, Bond angles and Dihedral angles:

The bond lengths data of the molecule have been given in Table 2. It is obtained that the C4-C11 bond (the carbon in cubane skeleton that linked to tetrazole ring) is shorter than other C-C bonds. And also, the bonds related to the carbons that attached to C4 are the longest in the structure. The molecular electrostatic potential (MEP) is the force acting on a positive test charge (a proton) located at a given point $p(x,y,z)$ in the vicinity of a molecule through the electrical charge cloud generated through the molecules electrons and nuclei. Despite the fact that the molecular charge distribution remains unperturbed through the external test charge (no polarization occurs) the electrostatic potential of a molecule is still a good guide in assessing the molecules reactivity towards positively or negatively charged reactants [9]. The MEP is typically visualized through mapping its values onto the surface reflecting the molecules boundaries [10]. The three-dimensional electrostatic potential maps of the

structures are shown in Figure 2. The red loops and the blue loops indicate negative and positive charge development for a particular system respectively. As can be seen from the figures the negative charge is located on the nitrogen elements of the tetrazole ring as expected due to the electron withdrawing character of theirs and positive charge is located on the carbon skeleton of the cubane section.

The bond angles data of the molecule have been given in Table 3. It is observed that the internal angles of the cubane section in the structure are approximately 90 degree, and the molecule is severely under pressure.

Natural Bond Orbital (NBO) population analysis:

The main objective is to study the nature of bonding in the 1H-tetrazolyl cubane, by using natural bond orbital analysis. The results from NBO computations can prepare the electronic structure details of the compound. The natural bond orbital calculation was carried out at B3LYP/6-311G(d,p) level. According to

calculation (Table 4), $\sigma(\text{C-C})$ bonds in cubane section are formed from about an $\text{SP}^{3.35}$ hybrid. And also, the $\sigma(\text{C-H})$ bonds are formed from an $\text{SP}^{2.3}$ hybrid on carbon atoms with S orbital on hydrogen atoms. So, the

hydrogen atoms of the cubane section of the molecule are acidic. It gets rid of the angular pressure in the cubane structure, the more P orbital of carbon atoms uses for forming C-C bonds.

Table 2: Bond lengths of 1H-tetrazolyl cubane.

Bonds (Å)	B3LYP/6-311G(d)	B3LYP/6-311G(d,p)	B3LYP/6-311G(2d,2p)
C1-C2	1.567	1.571	1.568
C2-C3	1.567	1.569	1.565
C3-C4	1.580	1.579	1.578
C4-C1	1.580	1.574	1.572
C1-C5	1.567	1.571	1.568
C2-C8	1.571	1.572	1.568
C3-C10	1.568	1.566	1.565
C4-C12	1.575	1.580	1.578
C4-C11	1.466	1.466	1.464
C5-C8	1.570	1.571	1.569
C8-C10	1.571	1.572	1.569
C10-C12	1.569	1.567	1.565
C12-C5	1.569	1.568	1.566
C1-H6	1.088	1.090	1.087
C2-H7	1.089	1.087	1.086
C3-H9	1.088	1.088	1.084
C5-H13	1.090	1.088	1.085
C8-H14	1.089	1.088	1.085
C10-H15	1.090	1.088	1.085
C12-H16	1.092	1.088	1.083
C11-N17	1.321	1.321	1.319
N17-N18	1.360	1.360	1.360
N18-N19	1.288	1.287	1.287
N19-N20	1.352	1.352	1.351
N20-C11	1.351	1.352	1.349
N20-H21	1.007	1.007	1.005

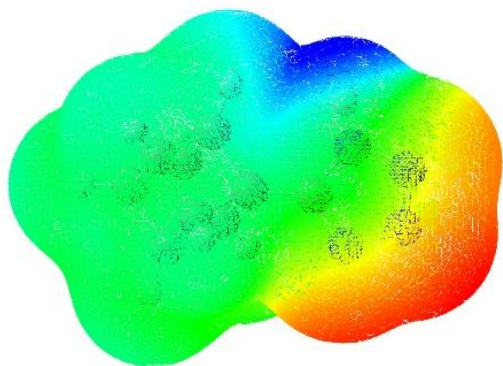


Figure 2: The 3-D electrostatic potential map of 1H-tetrazolyl cubane.

Infrared spectra:

The IR spectrum is one basic property of a compound, and also an effective measure to identify structures. Here, vibrational frequencies of the 1H-tetrazolyl cubane were calculated by using DFT method. Figure 3 provides IR spectra of the molecule at studied levels.

Harmonic frequencies (cm^{-1}), IR intensities (KM/Mole)

B3LYP/6-311G(d) level: -30.63 (7.53), 102.53 (2.79), 111.98 (5.16), 317.12 (0.48), 342.03 (0.13), 373.13 (5.82), 606.82 (64.14), 636.59 (5.22), 642.20 (0.93), 692.00 (2.33), 699.38 (0.07), 731.91 (11.68),

749.60 (2.43), 762.22 (0.72), 839.54 (0.26), 841.58 (0.07), 842.15 (0.20), 845.57 (0.01), 855.00 (6.86), 862.53 (7.03), 898.38 (2.12), 901.36 (2.86), 904.04 (2.35), 990.94 (0.02), 996.97 (0.68), 1019.97 (10.93), 1022.40 (1.29), 1045.89 (0.63), 1051.73 (38.10), 1069.91 (0.04), 1083.94 (14.49), 1093.68 (0.02), 1095.74 (0.27), 1128.09 (0.37), 1128.23 (0.01), 1145.17 (1.63), 1162.91 (0.02), 1175.53 (0.01), 1177.58 (0.01), 1209.48 (0.17), 1212.42 (0.72), 1234.24 (0.06), 1256.06 (6.03), 1259.89 (2.42), 1264.89 (4.65), 1282.41 (16.48), 1393.78 (11.86), 1408.24 (7.97), 1585.38 (84.10), 3083.81 (47.09), 3108.83 (15.50), 3113.75 (37.31), 3120.62 (79.73), 3121.59 (45.29), 3128.17 (67.66), 3138.30 (21.38), 3668.97 (52.16).

Table 3: Bond angles and dihedral angles of 1H-tetrazolyl cubane.

Bond angles (degree)	B3LYP/6-311G(d)	B3LYP/6-311G(d,p)	B3LYP/6-311G(2d,2p)	Bond angles (degree)	B3LYP/6-311G(d)	B3LYP/6-311G(d,p)	B3LYP/6-311G(2d,2p)
C1-C2-C3	90.168	90.372	90.389	C3-C10-C8	89.962	90.015	89.979
C2-C3-C4	90.288	89.822	89.848	C3-C10-C12	90.429	90.199	90.185
C3-C4-C1	89.230	89.881	89.788	C3-C10-H15	125.015	125.050	125.042
C4-C1-C2	90.314	89.923	89.972	C10-C3-H9	126.209	125.877	125.797
C4-C1-H6	123.519	125.765	125.677	C4-C12-C10	89.983	90.256	90.274
C2-C1-H6	125.784	125.037	128.081	C4-C12-C5	89.972	89.830	89.821
C4-C1-C5	89.877	89.973	89.981	C4-C12-H16	125.726	123.543	123.583
C2-C1-C5	90.149	90.007	89.974	C12-C4-C11	127.043	124.791	124.869
C1-C2-H7	125.009	124.860	124.914	C10-C12-H16	125.026	125.878	125.873
C3-C2-H7	124.995	125.121	125.026	C5-C12-H16	125.050	126.131	126.156
C1-C2-C8	89.963	89.989	90.059	C12-C5-H13	124.850	125.097	125.066
C3-C2-C8	89.970	89.945	90.000	C8-C5-H13	125.568	125.555	125.558
C2-C3-H9	125.826	126.134	126.193	C5-C8-H14	125.338	125.294	125.281
C4-C3-H9	123.512	123.552	123.579	C10-C8-H14	125.239	125.471	125.443
C2-C3-C10	90.170	90.172	90.142	C8-C10-H15	125.561	125.642	125.671
C4-C3-C10	89.845	90.291	90.289	C12-C10-H15	124.934	124.986	124.956
C3-C4-C11	124.804	124.808	124.902	C4-C11-N17	126.903	126.915	126.837
C1-C4-C11	124.826	126.895	126.802	C4-C11-N20	125.840	125.814	125.765
C1-C4-C12	89.738	89.826	89.815	C11-N20-H21	130.423	130.328	130.257
C3-C4-C12	89.737	89.254	89.252	N19-N20-H21	120.351	120.554	120.593
C5-C8-C10	89.925	89.930	89.885	C11-N17-N18	106.327	106.343	106.285
C8-C10-C12	90.010	89.947	90.009	N17-N18-N19	111.446	111.441	111.382
C10-C12-C5	90.030	90.213	90.123	N18-N19-N20	105.744	105.827	105.827
C12-C5-C8	90.033	89.910	89.983	N19-N20-C11	109.226	109.118	109.150
C1-C5-C12	90.411	90.369	90.380	N20-C11-N17	107.257	107.271	107.398
C1-C5-C8	89.993	90.029	90.031	C1-C4-C11-N17	58.753	179.993	180.000
C1-C5-H13	125.067	124.924	124.891	C3-C4-C11-N17	-58.871	-58.780	-58.910
C5-C1-H6	126.223	125.058	125.085	C12-C4-C11-N17	179.964	58.847	58.913
C2-C8-C5	89.894	89.972	89.935	C1-C4-C11-N20	-121.190	-0.027	-0.042
C2-C8-C10	89.898	89.869	89.879	C3-C4-C11-N20	121.186	121.209	121.037
C2-C8-H14	125.416	125.191	125.283	C12-C4-C11-N20	1.845	-121.164	-121.141
C8-C2-H7	125.718	125.596	125.536	C4-C11-N20-H21	-0.016	-0.016	1.946

Table 4: Natural bond orbital population analysis of 1H-tetrazolyl cubane calculated at B3LYP/6-311G(d,p) method.

Bonds	Occupancy	Population/Bond orbital/Hybrids
C1-C2	1.97746	50.69% C1 (SP ^{3.28}), 49.31% C2 (SP ^{3.33})
C1-C4	1.97027	48.54% C1 (SP ^{3.23}), 51.46% C4 (SP ^{3.36})
C1-C5	1.97746	50.69% C1 (SP ^{3.28}), 49.31% C5 (SP ^{3.33})
C1-H6	1.99224	60.84% C1 (SP ^{2.43}), 39.16% H6 (S)
C2-C3	1.97717	49.97% C2 (SP ^{3.28}), 50.03% C3 (SP ^{3.3})
C2-H7	1.99157	61.12% C2 (SP ^{2.38}), 38.88% H7 (S)
C2-C8	1.97954	50.25% C2 (SP ^{3.26}), 49.75% C8 (SP ^{3.31})
C3-C4	1.95298	47.68% C3 (SP ^{3.39}), 52.32% C4 (SP ^{3.47})
C3-H9	1.99144	61.51% C3 (SP ^{2.34}), 38.49% H9 (S)
C3-C10	1.97854	50.28% C3 (SP ^{3.24}), 49.72% C10 (SP ^{3.3})
C4-C11	1.97547	49.51% C4 (SP ^{2.12}), 50.49% C11 (SP ^{1.48})
C4-C12	1.95299	52.32% C4 (SP ^{3.47}), 47.68% C12 (SP ^{3.39})
C5-C8	1.97954	50.25% C5 (SP ^{3.26}), 49.75% C8 (SP ^{3.31})
C5-C12	1.97717	49.97% C5 (SP ^{3.28}), 50.03% C12 (SP ^{3.3})
C5-H13	1.99157	61.12% C5 (SP ^{2.38}), 38.88% H13 (S)
C8-C10	1.97989	50.07% C8 (SP ^{3.28}), 49.93% C10 (SP ^{3.3})
C8-H14	1.99191	61.06% C8 (SP ^{2.36}), 38.94% H14 (S)
C10-C12	1.97854	49.72% C10 (SP ^{3.3}), 50.28% C12 (SP ^{3.24})
C10-H15	1.99172	61.23% C10 (SP ^{2.36}), 38.77% H15 (S)
C11-N17	1.98206	43.14% C11 (SP ^{2.15}), 56.86% N17 (SP ^{1.78})
C11-N17	1.80925	40.55% C11 (P), 59.45% N17 (P)
C11-N20	1.98968	38.01% C11 (SP ^{2.61}), 61.99% N20 (SP ^{1.56})
C12-H16	1.99144	61.51% C12 (SP ^{2.34}), 38.49% H16 (S)
N17-N18	1.98030	50.37% N17 (SP ^{3.03}), 49.63% N18 (SP ^{2.78})
N18-N19	1.99065	48.87% N18 (SP ^{2.44}), 51.13% N19 (SP ^{2.23})
N18-N19	1.91057	48.27% N18 (P), 51.73% N19 (P)
N19-N20	1.98785	44.5% N19 (SP ^{3.39}), 55.5% N20 (SP ^{2.39})
N20-H21	1.99025	71.32% N20 (SP ^{2.19}), 28.68% H21 (S)

B3LYP/6-311G(d,p) level: -30.07 (7.41), 102.54 (2.77), 111.12 (5.15), 316.92 (0.45), 342.12 (0.17), 373.18 (5.77), 607.75 (57.62), 634.73 (5.53), 640.39 (0.91), 690.60 (2.13), 698.04 (0.07), 730.74 (10.96), 748.70 (2.37), 761.07 (0.44), 838.20 (0.25), 840.16 (0.06), 840.34 (0.18), 844.28 (0.005), 854.09 (6.76), 861.44 (7.01), 897.58 (2.25), 900.44 (2.82), 903.22 (2.40), 991.03 (0.01), 996.80 (0.56), 1019.30 (9.55), 1020.97 (2.21), 1042.80 (2.96), 1045.55 (37.12), 1067.49 (0.04), 1082.11 (14.07), 1091.20 (0.02), 1093.53 (0.40), 1124.95 (0.36), 1125.02 (0.01), 1143.62 (1.79), 1162.47 (0.02), 1173.83 (0.01), 1175.88 (0.01), 1206.41 (0.15), 1209.48 (0.70), 1230.48 (0.10), 1252.10 (6.11), 1255.65 (2.12), 1260.15 (4.19), 1280.50 (17.62), 1389.43 (6.02), 1403.72 (14.43), 1579.82 (82.50), 3085.26 (40.71), 3109.28 (13.11), 3113.82 (31.48), 3120.33 (68.32), 3121.33 (33.54), 3127.25 (54.50), 3136.76 (17.57), 3654.92 (65.78).

B3LYP/6-311G(2d,2p) level: -28.00 (6.86), 104.23 (6.70), 111.64 (4.94), 316.25 (0.40), 343.69 (0.06), 375.01 (5.77), 553.89 (60.12), 635.30 (0.43), 642.28 (0.91), 690.06 (1.17), 697.55 (0.06), 733.32 (7.32), 747.29 (2.39), 764.24 (0.13), 836.27 (0.22), 838.35 (0.03), 839.38 (0.21), 842.05 (0.01), 852.61 (6.54), 859.40 (6.99), 896.40 (2.05), 898.34 (2.45), 900.80 (2.29), 989.98 (0.004), 995.86 (0.77), 1015.76 (7.14), 1019.28 (6.62), 1040.55 (28.78), 1047.64 (8.59), 1068.00 (0.04), 1080.93 (15.08), 1092.57 (0.02), 1094.65 (0.34), 1128.31 (0.03), 1128.57 (0.33), 1142.96 (1.51), 1167.03 (0.02), 1175.17 (0.004), 1177.60 (0.01), 1207.09 (0.09), 1210.52 (0.66), 1230.67 (0.11), 1254.54 (4.16), 1255.45 (4.98), 1260.47 (3.83), 1278.80 (10.43), 1383.73 (4.19),

1400.99 (15.05), 1573.73 (81.26), 3093.23 (36.03), 3128.46 (40.75), 3135.08 (51.76), 3144.48 (16.11),
3115.04 (12.55), 3120.71 (27.85), 3127.46 (55.34), 3662.27 (60.44).

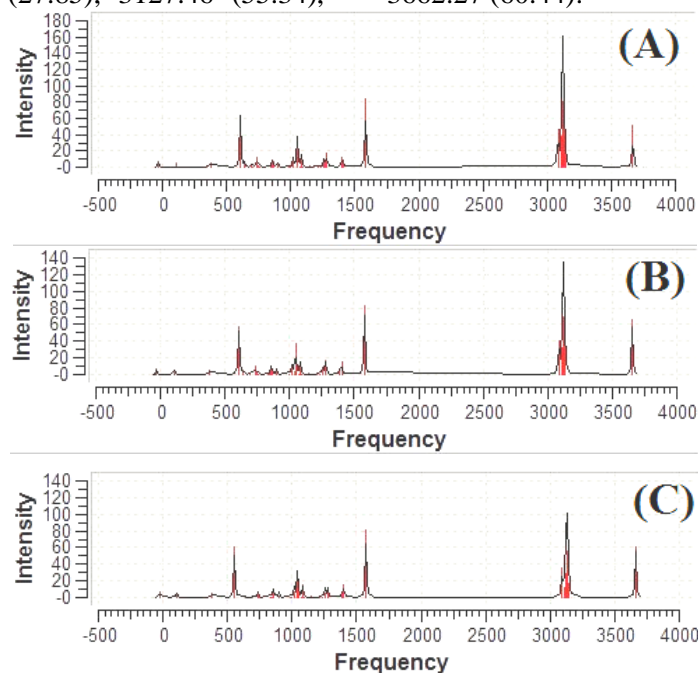


Figure 3: The IR spectra of 1H-tetrazolyl cubane in different theory methods A: B3LYP/6-311G(d), B: B3LYP/6-311G(d,p), C: B3LYP/6-311G(2d,2p).

NMR study:

The NMR analysis is an important property of a compound, and also an effective measure to identify structures. Here, nucleus shielding (ppm) for 1H-tetrazolyl cubane was calculated by using B3LYP/6-311G(d), B3LYP/6-311G(d,p) and B3LYP/6-311G(2d,2p) levels.

B3LYP/6-311G(d): -188.986 (N18), -137.291 (N19), -104.179 (N17), 22.410 (H21), 23.718 (C11), 25.052 (N20), 27.939 (H9), 27.940 (H16), 28.042 (H15), 28.119 (H7, H14), 28.148 (H6), 28.171 (H13), 126.278 (C3), 126.280 (C12), 129.602 (C4), 130.980 (C8), 131.425 (C1), 133.871 (C5), 133.872 (C2), 134.576 (C10).

B3LYP/6-311G(d,p): -189.626 (N18), -137.764 (N19), -104.107 (N17), 21.682 (H21), 23.588 (C11), 24.234 (N20), 27.621 (H6, H16), 27.749 (H9), 27.791 (H13), 27.854 (H7, H15), 27.869 (H14), 126.240 (C3), 126.244 (C12), 129.736 (C4), 130.896 (C8), 131.416 (C1), 133.840 (C5), 133.841 (C2), 134.521 (C10).

B3LYP/6-311G(2d,2p): -189.451 (N18), -136.114 (N19), -104.432 (N17), 21.107 (H21), 24.016 (C11), 24.209 (N20), 27.511 (H16), 27.619 (H6, H9), 27.628 (H7), 27.697 (H13, H15), 27.715 (H14), 126.707 (C3), 126.709 (C12), 129.876 (C4), 131.463 (C8), 131.622 (C1), 134.279 (C2, C5), 134.994 (C10).

Bond Dissociation Energy (BDE):

Bond dissociations investigation is essential and basic property for understanding the decomposition process of the High energy materials, since they are directly relevant to the stability and sensitivity of the high energy materials [11]. The energy required for bond hemolysis at 298 K temperature and 1 atmosphere pressure corresponds to the energy of reaction $A-B \rightarrow A^\bullet + B^\bullet$, which is the bond dissociation energy of the compound A-B by definition. Therefore, the bond dissociation energy can be given in terms of follow equation:

$$BDE_{(A-B)} = E_{(A^\bullet)} + E_{(B^\bullet)} - E_{(A-B)}$$

Where A-B corresponds for the structures, A^\bullet and B^\bullet stand for the corresponding product radicals after the bond dissociation, $BDE_{(A-B)}$ is the bond dissociation energy of bond A-B. The bond dissociation energy with ZPE correction can be calculated by follow equation:

$$BDE_{(A-B)ZPE} = BDE_{(A-B)} + \Delta ZPE$$

The bond dissociation energy of the 1H-tetrazolyl cubane was calculated at all the studied levels. Table 5 shows calculated total energy of the molecule and fragments at the equilibrium geometries and resulting BDEs at mentioned levels of theory. As seen from the table, the bond dissociation energy of the molecule is

about 113.8 kcal/mol. According to suggestion of Chung [12], the bond dissociation energy more than 20 kcal/mol corresponds for a compound to be considered

as a viable candidate of high energy density material (HEDM). Therefore, we can conclude that 1H-tetrazolyl cubane is a viable candidate of HEDMs.

Table 5: Calculated total energies of the 1H-tetrazolyl cubane and fragments, at the equilibrium geometries and resulting bond dissociation energies (BDE).

Methods	Formula	Parent energy (hartrees)	Fragment energy (hartrees)	1H- Tetrazole radical energy (hartrees)	BDE (kcal/mol)
B3LYP/6-311G(d)	C ₉ H ₈ N ₄	-566.48272	-308.72383	-257.57742	113.874
B3LYP/6-311G(d,p)	C ₉ H ₈ N ₄	-566.49749	-308.73579	-257.58037	113.786
B3LYP/6-311G(2d,2p)	C ₉ H ₈ N ₄	-566.51503	-308.74442	-257.58929	113.780

Key to the notation: B(L) stands for the radical obtained from B structure by removing the functional group at position L.

The frontier molecular orbital energies:

Table 6 shows the HOMO and LUMO energies (ϵ) of the molecule computed at B3LYP/6-311G(d), B3LYP/6-311G(d,p) and B3LYP/6-311G(2d,2p) levels of theory. The energy gap value, that is the difference between the LUMO and HOMO energy levels, is 0.25 a.u. at the studied methods.

Heats of formation, predicted densities and detonation of the structures:

The heats of formation (HOF) values were calculated at all studied levels and listed in the Table 7. In this study, isodesmic reaction method is employed. In isodesmic reaction, the numbers of bonds and bond types are preserved on both sides of the reaction [13]. The accuracy of HOF obtained computationally is conditioned by the reliability of HOF of the reference

compounds. The isodesmic reactions for HOF calculation are showed in Scheme 1.

For the isodesmic reactions, heat of reaction ΔH at 298.15 K can be calculated from the following equations:

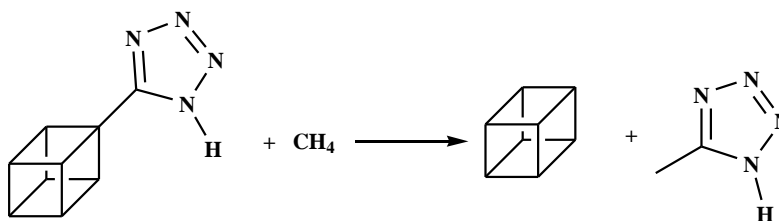
$$\begin{aligned} \Delta H_{298} &= \sum \Delta H_{f,P} - \sum \Delta H_{f,R} \\ \Delta H_{298.15K} &= \Delta E_{298.15K} + \Delta(PV) = \Delta E_0 + \Delta ZPE + \Delta H_T \\ &+ \Delta nRT \\ &= \sum \Delta H_{f,P} - \sum \Delta H_{f,R} \end{aligned}$$

Where $\Delta H_{f,P}$ and $\Delta H_{f,R}$ are the heats of formation of products and reactants at 298.15 K, respectively. ΔE_0 and ΔZPE correspond to the total energy difference and the zero point energy difference between products and reactants at 0 K, respectively. ΔH_T is the changes in thermal correction to enthalpies between products and reactants. $\Delta(PV)$ equals ΔnRT for reaction in gas phase. For isodesmic reactions, $\Delta n=0$. As seen from the table, the structure HOF is 920 kJ/mol.

Table 6: The HOMO and LUMO energies of 1H-tetrazolyl cubane.

Method	MOs number	HOMO orbital	HOMO (a.u.)	LUMO orbital	LUMO (a.u.)	$\Delta\epsilon$ (a.u.)
B3LYP/6-311G(d)	258	45 (A)	-0.27139	46 (A)	-0.02045	0.25094
B3LYP/6-311G(d,p)	282	45 (A)	-0.27179	46 (A)	-0.02134	0.25045
B3LYP/6-311G(2d,2p)	371	45 (A)	-0.27000	46 (A)	-0.01889	0.25111

$$\Delta\epsilon = \epsilon_{LUMO} - \epsilon_{HOMO}$$



Scheme 1: The isodesmic reaction for HOF calculation.

Furthermore, density (ρ), detonation velocity (D), and detonation pressure (P) are the important parameters to evaluate the explosive performances of

high energy materials and can be predicted by the following empirical Kamlet-Jacob equations [14]:

$$\begin{aligned} D &= 1.01(NM^{1/2}Q^{1/2})^{1/2}(1+1.3\rho) \\ P &= 1.558\rho^2NM^{1/2}Q^{1/2} \end{aligned}$$

parameters	Stoichiometric ratio		
	$c \geq 2a + b/2$	$2a + b/2 > c \geq b/2$	$b/2 > c$
N	$(b + 2c + 2d)/4MW$	$(b + 2c + 2d)/4MW$	$(b + d)/2MW$
M	$4MW/(b + 2c + 2d)$	$(56d + 88c - 8b)/(b + 2c + 2d)$	$(2b + 28d + 32c)/(b + d)$
Q	$(28.9b + 94.05a + 0.239\Delta H_f^\circ)/MW$	$[28.9b + 94.05(c/2 - b/4) + 0.239\Delta H_f^\circ]/MW$	$(57.8c + 0.239\Delta H_f^\circ)/MW$

Where D: detonation velocity in km/s, P: detonation pressure in GPa, ρ : density of a compound in g/cm^3 , N: moles of gaseous detonation products per gram of explosive (in mol/g), M: average molecular weight of

gaseous products (in g/mol), Q: chemical energy of detonation in kJ/g. Table 7 collects the predicted V, ρ , Q, D and P of the structures. As seen from the table, 1H-tetrazolyl cubane has good detonation properties.

Table 7: HOFs, predicted densities and detonation properties of 1H-tetrazolyl cubane.

Methods	OB ₁₀₀	HOF (kJ/mol)	Q (kJ/g)	V* (cm^3/mol)	ρ (g/cm^3)	D (km/s)	P (GPa)
B3LYP/6-311G(d)	111.58	920.137	1278.006	126.877	1.356	5.630	11.663
B3LYP/6-311G(d,p)	111.58	920.025	1277.850	116.714	1.474	5.943	13.781
B3LYP/6-311G(2d,2p)	111.58	919.783	1277.514	96.260	1.788	6.774	20.275

*Average value from 100 single-point volume calculations at the B3LYP/6-311G(d,p) level.

Q: Heat of explosion, V: Volume of explosion, D: Velocity of detonation, P: Pressure of explosion.

Conclusion

In the present work, stability of 1H-tetrazolyl cubane as potential candidate for high energy density materials (HEDMs) has been investigated computationally by using quantum chemical treatment. Full geometrical optimization of the structure was performed using density functional theory (DFT, B3LYP) at the levels of 6-311G(d), 6-311G(d,p), 6-311G(2d,2p). Introduction of tetrazolyl group into cubane system slightly affects the BDE and HOF. The detonation performance data are calculated according to the HOFs calculated by DFT theory. Also, it concluded that the structure is a viable candidate of high energy density materials (HEDMs).

Computational methods

All computational studies were performed with the Gaussian 03 package [15] using the B3LYP method with 6-311G(d), 6-311G(d,p) and 6-311G(2d,2p) basis sets. The term of B3LYP consists of the Vosko, Wilk, Nusair (VWN3) local correlation functional [16] and Lee, Yang, Parr (LYP) correlation correction functional [17, 18]. All computational sets were used as implemented in the Gaussian computational study. The geometry of 1H-tetrazolyl cubane was optimized without any structural or symmetry restrictions. For comparing of the bond strengths, hemolytic bond dissociation energy (BDE) calculations were performed the mentioned levels. The studied methods

were used to predict the HOFs of all molecules via isodesmic reactions. Vibrational analyses without any symmetry constraints were done for each set of calculations. Theoretical calculations have been performed in the gas phase [19]. An efficient and convenient statistics average method was worked out to predict the crystalline densities of all derivatives. To calculate the densities of 1h-tetrazolyl cubane, the molecular volume data was required. The molecular volume V was defined as inside a contour of 0.001 electrons/bohr³ density. The computational molecular density ρ ($\rho = M/V$, where M = molecular weight) was also calculated. Oxygen balance (OB₁₀₀) is an expression that is used to indicate the degree to which an explosive can be oxidized. OB₁₀₀ was calculated as follows:

$$OB\% = \frac{-1600}{\text{Mol. wt}} \times \left(2a + \frac{b}{2} - c \right)$$

Where: a = number of atoms of carbon, b = number of atoms of hydrogen, c = number of atoms of oxygen.

References

- [1] Eaton, P. E.; Cole, Jr., T. W. *J. Am. Chem. Soc.* **1964**, *86*, 3157.
- [2] Zhang, M.; Eaton, P. E.; Gilardi, R. *Angew. Chem. Int. Ed.* **2000**, *39*, 401.
- [3] Jursic, B. S. *J. Mol. Struct.* **2000**, *499*, 137.
- [4] Mahkam, M.; Nabati, M.; Latifpour, A.; Aboudi, J. *Des. Monomers Polym.* **2014**, *17*, 453.
- [5] Mahkam, M.; Namazifar, Z.; Nabati, M.; Aboudi, J. *Iran. J. Org. Chem.* **2014**, *6*, 1217.

- [6] Nabati, M.; Mahkam, M. *Iran. Chem. Commun.* **2014**, 2, 164.
- [7] Babler, J. H.; Sarussi, S. J. *J. Org. Chem.* **1983**, 48, 4416.
- [8] Derrick Clive, L. J.; Angoh, A. G.; Bennett S. M. *J. Org. Chem.* **1987**, 52, 1339.
- [9] Türker, L. *J. Mol. Struct. (Theochem)* **2004**, 681, 15.
- [10] Glukhovtsev, M. N. *J. Chem. Educ.* **1997**, 74, 132.
- [11] Jiao, H.; Schleyer, P. R. *J. Phys. Org. Chem.* **1998**, 11, 655.
- [12] Chung, G. S.; Schimidt, M. W.; Gordon, M. S. *J. Phys. Chem. A* **2000**, 104, 5647.
- [13] Politzer, P.; Martinez, J.; Murray, J. S.; Concha, M. *C. Mol. Phys.* **2009**, 107, 2095.
- [14] Kamlet, M. J.; Jacobs, S. J. *J. Chem. Phys.* **1968**, 48, 23.
- [15] Frisch, M. J.; Trucks, G. W.; Schlegel, H. B.; Scuseria, G. E.; Robb, M. A.; Cheeseman, J. R.; Montgomery Jr., J. A.; Vreven, T.; Kudin, K. N.; Burant, J. C.; Millam, J. M.; Iyengar, S. S.; Tomasi, J.; Barone, V.; Mennucci, B.; Cossi, M.; Scalmani, G.; Rega, N.; Petersson, G. A.; Nakatsuji, H.; Hada, M.; Ehara, M.; Toyota, K.; Fukuda, R.; Hasegawa, J.; Ishida, M.; Nakajima, T.; Honda, Y.; Kitao, O.; Nakai, H.; Klene, M.; Li, X.; Knox, J. E.; Hratchian, H. P.; Cross, J. B.; Adamo, C.; Jaramillo, J.; Gomperts, R.; Stratmann, R. E.; Yazyev, O.; Austin, A. J.; Cammi, R.; Pomelli, C.; Ochterski, J. W.; Ayala, P. Y.; Morokuma, K.; Voth, G. A.; Salvador, P.; Dannenberg, J. J.; Zakrzewski, V. G.; Dapprich, S.; Daniels, A. D.; Strain, M. C.; Farkas, O.; Malick, D. K.; Rabuck, A. D.; Raghavachari, K.; Foresman, J. B.; Ortiz, J. V.; Cui, Q.; Baboul, A. G.; Clifford, S.; Cioslowski, J.; Stefanov, B. B.; Liu, G.; Liashenko, A.; Piskorz, P.; Komaromi, I.; Martin, R. L.; Fox, D. J.; Keith, T.; Al-Laham, M. A.; Peng, C. Y.; Nanayakkara, A.; Challacombe, M.; Gill, P. M. W.; Johnson, B.; Chen, W.; Wong, M. W.; Gonzalez, C.; Pople, J. A. *Gaussian 03. Revision B.01*. Gaussian Inc. Wallingford. CT. **2004**.
- [16] Vosko, S. H.; Wilk, L.; Nusair, M. *Can. J. Phys.* **1980**, 58, 1200.
- [17] Lee, C.; Yang, W.; Parr, R. G. *Phys. Rev. B* **1988**, 37, 785.
- [18] Miehlich, B.; Savin, A.; Stoll, H.; Preuss, H. *Chem. Phys. Lett.* **1989**, 157, 200.
- [19] Nabati, M.; Mahkam, M. *Silicon* **2015**, 7, in press.